HEP'99 # 5_77
Submitted to Pa 5, 6
Pl 5, 6

DELPHI 99-129 CONF 316
15 June 1999

A Study of the Lorentz Structure in Tau Decays

Preliminary

DELPHI Collaboration

Paper submitted to the HEP'99 Conference
Tampere, Finland, July 15-21

A Study of the Lorentz Structure in Tau Decays

Preliminary

DELPHI Collaboration

P. Seager [1], **I. Boyko** [2], **M. Chizhov** [3], **P. Ratoff** [1]

Abstract

This paper describes a measurement of the Michel parameters, η, ρ, ξ, $\xi\delta$, and the average ν_τ helicity, h_{ν_τ}, in τ lepton decays together with limits placed on tensor couplings in the weak charged current. The $\tau^+\tau^-$ pairs were produced at the LEP e^+e^- collider at CERN from 1992 through 1995 in the DELPHI detector. These parameters were extracted in a simultaneous fit to the two-dimensional momentum spectra of leptonic and semi-leptonic τ decays.

Assuming lepton universality in the decays of the τ the measured values of the parameters were: $\eta_l = -0.005 \pm 0.036 \pm 0.037$, $\rho_l = 0.775 \pm 0.023 \pm 0.020$, $\xi_l = 0.929 \pm 0.070 \pm 0.030$, $\xi_l\delta_l = 0.779 \pm 0.070 \pm 0.028$, $h_{\nu_\tau} = -0.997 \pm 0.027 \pm 0.011$. The strength of the tensor coupling was measured to be $\kappa_\tau^W = -0.029 \pm 0.036 \pm 0.018$. The first error is statistical and the second error is systematic in all cases. The results are consistent with the $V - A$ structure of the weak charged current in decays of the τ lepton.

[1] Lancaster University, UK.

[2] JINR, Dubna, Russian Federation.

[3] Sofia University, Bulgaria.

1 Introduction

The Michel parameters [1], η, ρ, ξ, and $\xi\delta$, are a set of experimentally accessible parameters which are bilinear combinations of ten complex coupling constants describing the couplings in the charged current decay of charged leptons. The Standard Model makes a specific prediction about the exact nature of the structure of the weak charged current. τ leptons provide a unique environment in which to verify this prediction. Not only is the large mass of the τ lepton (and thus an extensive range of decay channels) strong motivation to search for deviations from the Standard Model but the τ also offers the possibility to test the hypothesis of lepton universality.

The Michel parameters in τ decays have been extensively studied by many experiments both at e^+e^- colliders running at the Z pole and at low energy machines [2, 3, 4, 5, 6, 7]. This paper describes an analysis of τ decays using both the purely leptonic and the semi-leptonic (hadronic) decay modes, the latter being selected without any attempt to identify the specific decay channel. In grouping together all the semi-leptonic decays one can obtain a relatively high efficiency and purity at the expense of a loss of sensitivity to the relevant parameters. This sensitivity is recuperated by splitting the semi-leptonic decay candidates into bins of invariant mass of the hadronic decay products, each bin being separately dominated by a different τ decay mode.

Further constraints on η can be imposed by using measurements of the leptonic branching ratios of the τ lepton.

The measurement of the Michel parameters in the purely leptonic decay modes of the τ allows limits to be placed on new physics. The large number of Michel parameters, however, reduces the experimental sensitivity in placing these limits. Moreover, the Michel parameterisation does not cover the full variety of possible interactions; in particular it does not include terms with derivatives. However, a complementary test of a special type of new interaction is presented. In addition to testing new couplings of the W boson with leptonic currents that conserve fermion chiralities, the possibility of anomalous W coupling to a leptonic charged tensor current is explored.

2 The Michel parameters and ν_τ helicity

The most general form for the matrix element, $\mathcal{M}$, describing the leptonic decay $\tau \to l\overline{\nu}_l\nu_\tau$, can be written as follows [8, 9, 10]:

$$\mathcal{M} \;=\; \frac{4G}{\sqrt{2}} \sum_{\substack{N=S,V,T \\ i,j=L,R}} g_{ij}^N \left\langle \overline{u}_{l_i} \,\middle|\, \Gamma^N \,\middle|\, (v_{\overline{\nu}_l})_n \right\rangle \left\langle (\overline{u}_{\nu_\tau})_m \,|\, \Gamma_N \,|\, u_{\tau_j} \right\rangle, \tag{1}$$

which is characterised by spinors of definite handedness. G is the Fermi coupling constant and the Γ_N represent the various forms of the weak charged current allowed by Lorentz invariance. The n and m in equation 1 are the helicities of the neutrinos which are uniquely determined by a given N, i and j. In the case of vector and axial-vector interactions the helicity of the neutrino is equal to the helicity of its associated charged lepton, while it is the opposite in the case of scalar, pseudoscalar and tensor interactions.

The g_{ij}^N's here are the complex coupling constants. There are 12 of these but, excluding the possibility of the existence of a vector boson carrying a chiral charge, two of the

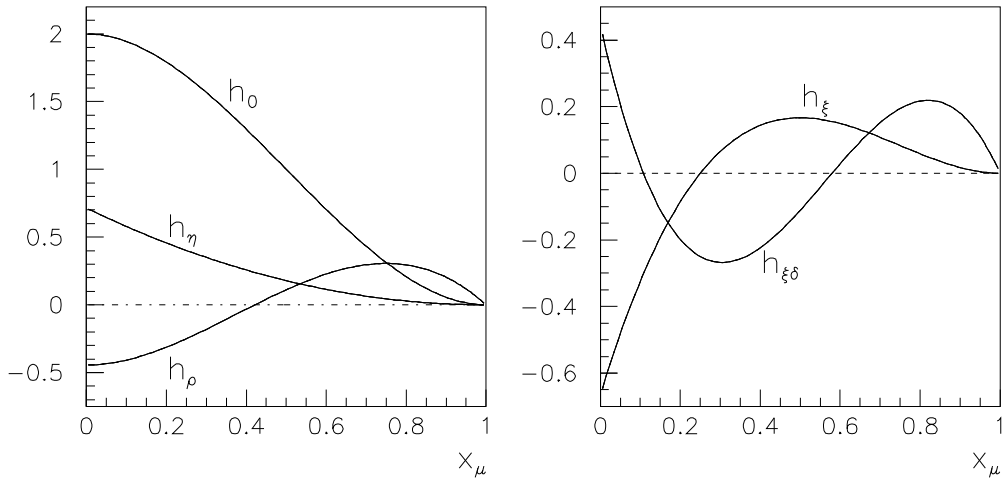

Figure 1: Polynomial functions for the $\tau \to \mu\overline{\nu}_\mu\nu_\tau$ decay channel. Effects of the finite mass of the μ and radiative corrections are not included in the plots.

constants, g^T_{LL} and g^T_{RR}, are identically zero. As the couplings can be complex, with an arbitrary phase, there are 19 independent parameters. The Standard Model $V-A$ structure for the weak charged current predicts that $g^V_{LL}=1$ with all other couplings being identically zero.

The matrix element (1) can now be used to form the decay distribution of the leptonic τ decay in terms of the normalised energy of the daughter lepton $x_l = E_l/E_{beam}$ as follows:

$$\begin{aligned}\frac{1}{\Gamma}\frac{d\Gamma}{dx_l} &= H_0(x_l) - \mathcal{P}_\tau H_1(x_l) \\ &= h_0(x_l) + \eta h_\eta(x_l) + \rho h_\rho(x_l) \\ &\quad -\mathcal{P}_\tau\left(\xi h_\xi(x_l) + \xi\delta h_{\xi\delta}(x_l)\right) \end{aligned} \tag{2}$$

where $\mathcal{P}_\tau$ is the average τ polarisation. The h's at Born level are polynomials and are illustrated in figure 1. The Michel parameters, η, ρ, ξ and $\xi\delta$, are bilinear combinations of the complex coupling constants [1]. With the Standard Model predictions for these coupling constants the Michel parameters η, ρ, ξ and $\xi\delta$ take on the values 0, $\frac{3}{4}$, 1 and $\frac{3}{4}$ respectively.

It is instructive to consider the physical significance of some of these parameters. A single measurement of ρ does not constrain the form of the interaction. For example, if ρ were to be measured to be $\frac{3}{4}$, as is the case for the Standard Model prediction, then this would not rule out any combination of the six couplings g^S_{LL}, g^S_{LR}, g^S_{RL}, g^S_{RR}, g^V_{RR}, g^V_{LL} with the other couplings being zero. Indeed a $V+A$ structure would have a value of ρ of $\frac{3}{4}$. In this case one must examine the other parameters. For example, a $V+A$ structure would mean that the parameter ξ would be equal to -1.

The η parameter is of particular interest. It is sensitive to the low energy part of the decay lepton spectrum. It is practically impossible to measure η for $\tau \to e\nu_\tau\overline{\nu}_e$ decays because of a heavily suppressive factor of $\frac{m_e}{m_\tau}$ in the h_η polynomial. This suppressive factor is of the order of $\simeq 1/17$ for $\tau \to \mu\nu_\tau\overline{\nu}_\mu$ and hence all sensitivity to η is in this channel.

η receives contributions from the interference between *vector and scalar* and *vector and tensor* interactions and is therefore particularly sensitive to non $V-A$ interactions. If $\eta \neq 0$ there would be two or more different couplings with opposite chiralities for the charged leptons and this would result in non-maximal parity and charge conjugation violation. In this case, if $V-A$ is assumed to be dominant, then the second coupling would be a Higgs type coupling with a right handed τ and and charged lepton, l (where $l = e, \mu$). [11].

Under the assumption of lepton universality the leptonic decay rates of the τ lepton may be affected by the exchange of a non-standard charged scalar particle [13] and these effects can be conveniently expressed through the parameter η [14, 15]. The generalized leptonic decay rate of the τ becomes

$$\Gamma(\tau \rightarrow l\nu_\tau\overline{\nu}_l) = \frac{G_{l\tau}^2 m_\tau^5}{192\pi^3}\left[f(\frac{m_l^2}{m_\tau^2}) + 4\frac{m_l}{m_\tau}g(\frac{m_l^2}{m_\tau^2})\eta\right] r_{RC}^\tau \tag{3}$$

where $G_{l\tau}$ is the coupling of the τ to a lepton of type l, and equals the Fermi coupling constant if lepton universality holds. The functions f and g are phase space factors and the quantity r_{RC}^τ is a factor due to electroweak radiative corrections, which to a good approximation has the value 0.9960 for both leptonic decay modes of the τ. The factor $f(\frac{m_l^2}{m_\tau^2})$ is equal to 1.0000 for electrons and 0.9726 for muons. However, the function $4\frac{m_e}{m_\tau}g(\frac{m_e^2}{m_\tau^2})$ equals 0.001, whereas the value of $4\frac{m_\mu}{m_\tau}g(\frac{m_\mu^2}{m_\tau^2})$ is relatively large, equal to 0.2168. Hence, a stringent limit on η in $\tau \rightarrow \mu$ decays can be set on the basis of the branching ratio measurements, since to a good approximation

$$\frac{Br(\tau \rightarrow \mu\nu_\tau\overline{\nu}_\mu)}{Br(\tau \rightarrow e\nu_\tau\overline{\nu}_e)} \;=\; f\Big(\frac{m_\mu^2}{m_\tau^2}\Big) + 4\frac{m_\mu}{m_\tau}g\Big(\frac{m_\mu^2}{m_\tau^2}\Big)\eta. \tag{4}$$

One can define the variable, P_R^τ, as the probability that a right handed τ will decay into a lepton of either handedness [11]. This variable is related to the Michel parameters ξ and $\xi\delta$ and to five of the complex coupling constants in the following way:

$$\begin{aligned} P_R^\tau &= \frac{1}{4}|g_{RR}^S|^2 + \frac{1}{4}|g_{LR}^S|^2 + |g_{RR}^V|^2 + |g_{LR}^V|^2 + 3|g_{LR}^T|^2 \\ &= \frac{1}{2}[1 + \frac{1}{9}(3\xi - 16\xi\delta)]. \end{aligned} \tag{5}$$

Hence the quantity P_R^τ is a measure of the contributions of five coupling constants involving right handed τ's. One can therefore see that measuring the parameters ξ and $\xi\delta$ is of considerable interest in studying the structure of the weak charged currents.

As only the relative weights of the different couplings, g_{ij}^N, are of interest, the couplings can be normalised by taking out a common factor which is determined by the total decay rate [11, 12]:

$$\Gamma = \frac{A m_\tau^5 G_F^2}{16 \cdot 192\pi^3}, \tag{6}$$

assuming Standard Model couplings, where

$$\begin{aligned} A \;\equiv\; & 4(|g_{RR}^S|^2 + |g_{LR}^S|^2 + |g_{RL}^S|^2 + |g_{LL}^S|^2) + 48(|g_{LR}^T|^2 + |g_{RL}^T|^2) \\ & + 16(|g_{RR}^V|^2 + |g_{LR}^V|^2 + |g_{RL}^V|^2 + |g_{LL}^V|^2) \;\equiv\; 16. \end{aligned} \tag{7}$$

One can now calculate the reduced coupling constants. These are defined to be $f_{ij}^N \equiv g_{ij}^N/\max(g_{ij}^N)$. It can be seen from the above normalisation condition that the maximum values that the coupling constants g_{ij}^N can take are 2, 1 and $1/\sqrt{3}$ for $N = S, V$ and T respectively. This relation will be used later in this text in order to place limits on the reduced coupling constants. The f_{ij}^N couplings have a simple physical interpretation in that $\left|f_{ij}^N\right|^2$ is equal to the relative probability for a j handed τ to decay into an i handed daughter lepton by the interaction Γ^N.

At this point it is worth noting that the Michel parameters are restricted by boundary conditions. The leptonic decay rate of the τ equation 2 has to be positive definite. Certain combinations of the Michel parameters lead to unphysical effects. It has been shown that [16] the following constraints must be satisfied:

$$0 \leq \rho \leq 1, \tag{8}$$

$$|\xi| \leq 3, \tag{9}$$

$$|\xi\delta| \leq \rho, \tag{10}$$

$$|7\xi\delta - 3\xi| \leq 9(1-\rho). \tag{11}$$

The first two conditions arise from the fact that the different couplings in the definitions of the Michel parameters occur in quadrature. The third constraint can be directly found if the high energy limit of the τ decay rate is demanded to be positive definite. The final constraint can be seen to satisfy the condition $0 \leq P_R^\tau \leq 1$ from equation 5. It is interesting to note that the Standard Model values of the Michel parameters are consistently right at the edge of the allowed regions (see figure 8).

The decay width of the semi-leptonic decays of the τ can be written, assuming vector and axial-vector couplings at the decay vertices, as the following:

$$\begin{aligned} \frac{1}{\Gamma}\frac{d\Gamma}{dx} &= H_0(x) + \mathcal{P}_\tau H_1(x) \\ &= h_0(x) - h_{\nu_\tau}\mathcal{P}_\tau h_1(x) \end{aligned} \tag{12}$$

where x is a polarisation sensitive variable in each decay channel. For the case of $\tau \to \pi\nu_\tau$ this variable is $cos\theta^*$, the decay angle of the π in the τ rest frame, whilst for the two cases of $\tau \to \rho\nu_\tau$ and $\tau \to a_1\nu_\tau$ the variable used is the ω variable described in [17].

The h_{ν_τ} parameter can be shown to represent the helicity of the τ neutrino and can be expressed as follows:

$$h_{\nu_\tau} = \frac{2\mathrm{Re}(v_\tau a_\tau^*)}{|v_\tau|^2 + |a_\tau|^2} \tag{13}$$

where v_τ and a_τ are the vector and axial-vector couplings of the τ lepton to W bosons. Assuming that the vector boson exchanged in producing the $\tau^+\tau^-$ pair only involved vector and axial-vector type couplings then the helicities of the τ^+ and τ^- are almost 100% anti-correlated. This fact is used to construct the correlated spectra:

$$\frac{1}{\Gamma}\frac{d^2\Gamma}{dx_1 dx_2} = \frac{1+\mathcal{P}_\tau}{2}\left(H_0(x_1)-H_1(x_1)\right)\left(H_0(x_2)-H_1(x_2)\right) + \frac{1-\mathcal{P}_\tau}{2}\left(H_0(x_1)+H_1(x_1)\right)\left(H_0(x_2)+H_1(x_2)\right) \quad (14)$$

in terms of the polarisation sensitive variable x (which is decay channel dependent). The H_0's and H_1's are the polynomials described previously.

3 Anomalous tensor couplings

The Lagrangian for the leptonic decay of the τ can be written in the following way:

$$\mathcal{L} = \frac{g}{\sqrt{2}}\, W^\alpha \left\{\overline{\tau}\gamma_\alpha \frac{1-\gamma^5}{2}\nu + \frac{\kappa_\tau^W}{2m_\tau}\partial_\beta\left(\overline{\tau}\sigma_{\alpha\beta}\frac{1-\gamma^5}{2}\nu\right)\right\} + hc. \quad (15)$$

where W^α is the weak charged current of the leptonic decay products of the W boson and κ_τ^W is a parameter which controls the strength of the tensor coupling. The choice of such a kind of interaction to test for the existence of new physics is inspired by experiments with semi-leptonic decays of pions [18] and kaons [19], which show a deviation from the Standard Model which can be explained by the existence of an anomalous interaction with a tensor leptonic current [20]. Since the new interaction explicitly contains derivatives, its effect on the distortion of the energy spectrum of charged leptons in τ decays can not be described in terms of the known Michel parameters. Constraints will be placed on the parameter κ_τ^W from the analysis of both leptonic and semi-leptonic τ decays, fixing the Michel parameters to their Standard Model values. The inclusion of the semi-leptonic channels significantly increases the sensitivity to the new tensor coupling and imposes stricter constraints.

Beginning with the purely leptonic decays, the laboratory energy spectrum of the charged decay product can be expressed as follows:

$$\frac{\mathrm{d}\Gamma}{\mathrm{d}x_l} \propto f(x_l) + \mathcal{P}_\tau g(x_l), \quad (16)$$

where x_l is again the normalised momentum of the daughter lepton.

The expressions for $f(x_l)$ and $g(x_l)$, accounting for the new tensor interaction, were obtained in the rest frame of a decaying lepton [21]. Neglecting the mass of the final lepton and boosting these expressions along the τ flight direction for τ's produced in e^+e^- interactions at $\sqrt{s} = E_{beam}$ gives

$$\begin{aligned} f(x_l) &= 5 - 9x_l^2 + 4x_l^3 + 2\kappa_\tau^W(1-x_l^3), \\ g(x_l) &= 1 - 9x_l^2 + 8x_l^3 + 2\kappa_\tau^W(1-3x_l+2x_l^3). \end{aligned} \quad (17)$$

For the semi-leptonic decays of the τ, within the Born approximation, the tensor interaction does not contribute to the process $\tau \to \pi\nu_\tau$. Therefore, among the main τ lepton decay modes only $\tau \to \rho\nu_\tau \to (2\pi)\nu_\tau$ and $\tau \to a_1\nu_\tau \to (3\pi)\nu_\tau$ yield information about the new tensor interaction. To increase the sensitivity, the analysis is performed

using the two angular variables θ^* and ψ, where θ^* is the angle in the τ rest frame between the τ polarisation and the momentum of the final (pseudo) vector particle, and ψ denotes the spin 1 system helicity through the decay distribution of the hadronic system [17].

The τ decay to a particle of spin 1 and mass m and a neutrino has two amplitudes, A_L and A_T, representing longitudinal and transverse polarisation of the spin 1 particle. From the expression for the decay helicity amplitudes

$$\mathcal{M}_\lambda \propto \overline{\nu}(1+\gamma^5)\left[\gamma_\alpha - i\frac{\kappa_\tau^W}{2m_\tau}q_\beta\sigma_{\alpha\beta}\right]\tau\ \epsilon_\alpha^*(q,\lambda), \tag{18}$$

where ϵ_α^* is the polarisation vector of the spin 1 particle with momentum q and helicity λ, one gets:

$$\frac{A_T}{A_L} = \frac{\sqrt{2}m}{m_\tau}\ \frac{a_T}{a_L}, \tag{19}$$

where $a_T = 1 + \kappa_\tau^W/2$ and $a_L = 1 + (m^2/m_\tau^2)\kappa_\tau^W/2$. Therefore for $\tau \to (2\pi)\ \nu$ and $\tau \to (3\pi)\ \nu$:

$$\frac{\mathrm{d}^2N}{\mathrm{d}\cos\theta^*\ \mathrm{d}\cos\psi} \propto H^+(1+P_\tau) + H^-(1-P_\tau), \tag{20}$$

where H^+ and H^- are linear functions of a_T and a_L.

4 The DELPHI Detector

The DELPHI detector is described in detail elsewhere [22]. The following is a summary of the sub-detector units particularly relevant for this analysis. All these covered the full solid angle of the analysis except where specified. In the DELPHI reference frame the z-axis is taken along the direction of the e^- beam. The angle Θ is the polar angle defined with respect to the z-axis, ϕ is the azimuthal angle about this axis and r is the distance from this axis. The reconstruction of a charged particle trajectory in the barrel region of DELPHI resulted from a combination of the measurements in:

- the Vertex Detector (VD), made of three layers of silicon micro-strip modules, at radii of 6.3, 9.0 and 11.0 cm from the beam axis. The space point precision was about 8 μm in r-ϕ and varied from about 8 μm to 30 μm, depending on Θ, in r-z. The two track resolution was 100 μm in r-ϕ and 200 μm in r-z.

- the Inner Detector (ID), with an inner radius of 12 cm and an outer radius of 28 cm. A jet chamber measured 24 r-ϕ coordinates and provided track reconstruction. Its two track resolution in r-ϕ was 1 mm and its spatial precision 40 μm. It was surrounded by an outer part which served mainly for triggering purposes. This outer part was replaced for the 1995 data with a straw-tube detector containing much less material.

- the Time Projection Chamber (TPC), extending from 30 cm to 122 cm in radius. This was the main detector for the track reconstruction. It provided up to 16 space points for pattern recognition and ionisation information extracted from 192 wires. Every 60° in ϕ there was a boundary region between read-out sectors about 1° wide

which had no instrumentation. At $\cos\Theta = 0$ there was a cathode plane which caused a reduced tracking efficiency in the polar angle range $|\cos\Theta| < 0.035$. The TPC had a two track resolution of about 1.5 cm in r-ϕ and in z. The measurement of the ionisation deposition had a typical precision of $\pm 6\%$.

- the Outer Detector (OD) with 5 layers of drift cells at a radius of 2 m from the beam axis, sandwiched between the RICH and HPC sub-detectors described below. Each layer provided a space point with 110 μm precision in r-ϕ and about 5 cm precision in z.

These detectors were surrounded by a solenoidal magnet with a 1.2 Tesla field parallel to the z-axis. In addition to the detectors mentioned above, the identification of the τ decay products relied on:

- the barrel electromagnetic calorimeter, a High density Projection Chamber (HPC). This detector lay immediately outside the tracking detectors and inside the magnet coil. Eighteen radiation lengths deep for perpendicular incidence, its energy resolution was $\Delta E/E = 0.31/E^{0.44} \oplus 0.027$ where E is in units of GeV. It had a high granularity and provided a sampling of shower energies from nine layers in depth. It allowed a determination of the starting point of an electromagnetic shower with an accuracy of 0.6 mrad in polar angle and 3.1 mrad in azimuthal angle. The HPC had a modularity of 15° in azimuthal angle. Between modules there was a region with a width of about 1° in azimuth where the energy resolution was degraded.

- the Hadron Calorimeter (HCAL), sensitive to hadronic showers and minimum ionising particles. It was segmented in 4 layers in depth, with a granularity of 3.75° in polar angle and 2.96° in azimuthal angle. Lying outside the magnet solenoid, it had a depth of 110 cm of iron.

- the barrel Muon Chambers (MUB) consisting of two layers of drift chambers, the first one situated after 90 cm of iron and the second outside the hadron calorimeter. The acceptance in polar angle of the outer layer was slightly smaller than the other barrel detectors and covered the range $|\cos\Theta| < 0.602$. The polar angle range $0.602 < |\cos\Theta|$ was covered by the forward Muon Chambers (MUF) in certain azimuthal zones.

The DELPHI trigger was very efficient for τ final states due to the redundancy existing between its different components. From the comparison of the response of independent components, a trigger efficiency of $(99.98 \pm 0.01)\%$ has been derived.

5 Particle identification and energy calibration

The detector response was extensively studied using simulated data together with various test samples of real data where the identity of the particles was unambiguously known. Examples of such samples consisted of $e^+e^- \to e^+e^-$, and $e^+e^- \to \mu^+\mu^-$ events together with the radiative processes $e^+e^- \to e^+e^-\gamma$ and $e^+e^- \to \mu^+\mu^-\gamma$. Test samples using the redundancy of the detector were also used. An example of such a sample is $\tau \to \pi(n\pi^0)$, $(n > 0)$, selected by tagging the π^0 decay in the HPC. This sample was extensively used as a pure sample of charged hadrons to test the response of the calorimetry and muon chambers.

5.1 TPC ionisation measurement

The ionisation loss of a track as it travels through the TPC gives good separation between electrons and charged pions, particularly in the low momentum range. Because of the importance of this variable it was required that there were at least 28 anode wires used in the measurement. This reduced the sample by a small amount primarily due to tracks being close to the boundary regions of the TPC sectors where a narrow non-instrumented strip was located. The dE/dx pull variable, $\prod^{j}_{dE/dx}$, for a particular particle hypothesis (j = e, μ, π, K) is defined as

$$\prod^{j}_{dE/dx} = \frac{dE/dx_{meas} - dE/dx_{expt}(j)}{\sigma(dE/dx)} \tag{21}$$

where dE/dx_{meas} is the measured value, $dE/dx_{expt}(j)$ is the expected momentum dependent value for a hypothesis j and $\sigma(dE/dx)$ is the resolution of the measurement.

5.2 Electromagnetic calorimetry

The HPC electromagnetic calorimeter is used for e, γ and π^0 identification. For charged particles E_{ass} is the energy deposited by the track in the HPC. For electrons this energy should be (within experimental errors) equal to the measured value of the momentum. For hadrons the energy should be lower than the measured momentum as hadrons should traverse the HPC leaving either zero or a small amount of their energy. Muons, being minimum ionising particles, should go through the HPC depositing only a small amount of energy. On average they deposit 200 MeV uniformly in depth.

The ratio of the energy deposition in the HPC to the reconstructed momentum has a peak at one for electrons and a rising distribution towards zero for hadrons. The pull variable, $\prod_{E/p}$, is defined as

$$\prod_{E/p} = \frac{E_{ass}/p' - 1}{\sigma(E_{ass}/p')} \tag{22}$$

where p' is the momentum refit without the use of the OD, described in section 5.4 below, and $\sigma(E_{ass}/p')$ is the expected resolution for an electron of momentum p'. This variable gives particularly good separation at high momenta.

5.3 Hadron calorimetry and muon identification

The HCAL was used in particular for separating pions from muons. As muons travel through the HCAL they deposit a small amount of energy evenly through the 4 layers and travel on into the muon chambers whereas hadrons deposit all their energy late in the HPC and/or in the first layers of the HCAL so that they rarely penetrate through to the muon chambers. It follows therefore that the variable E_{hlay}, the average energy deposited in the HCAL per HCAL layer is constructed:

$$E_{hlay} = \frac{E_{HCAL}}{N_{layers}} \times sin^2\Theta \tag{23}$$

where E_{HCAL} is the total deposited energy in the HCAL; N_{layers} is the number of HCAL layers with an energy deposit and $sin^2\Theta$ smooths out the angular dependence of the

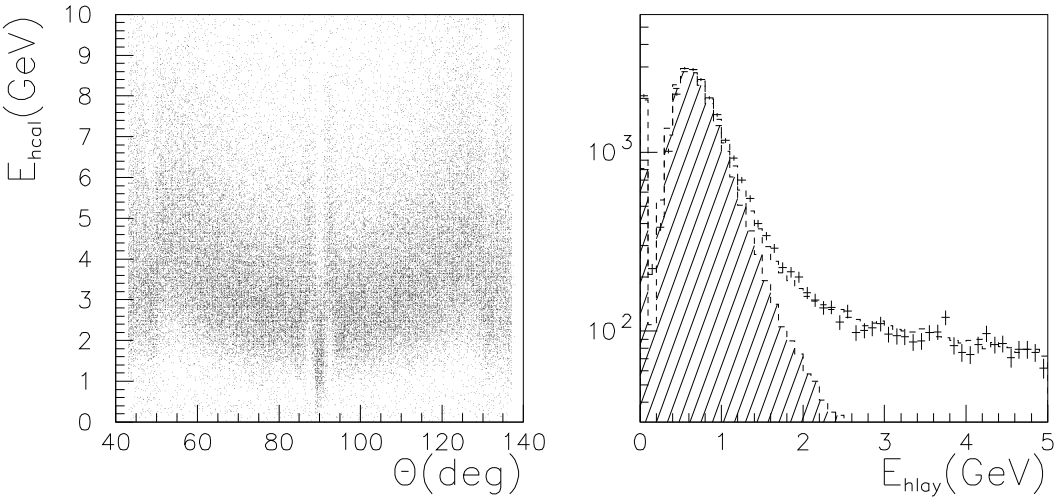

Figure 2: The HCAL response to muons (left plot) together with the variable E_{hlay} (right plot) for a sample of hadrons and muons in 1994 data (barrel region only). The points are the real data, the dashed histogram is the simulated sum of hadrons and muons and the hatched area is the simulated muons.

energy response of the HCAL (see figure 2). This variable provides good separation between muons and hadrons as can be seen in figure 2.

5.4 Momentum determination and scale

A good knowledge of the momentum and energy of charged particles is required for a Michel parameter analysis. This is especially true for the leptonic channels. As already mentioned the momentum is measured by tracking the particles in a magnetic field as they traverse the detector. The precision on the component of momentum transverse to the beam direction, p_t, obtained with the DELPHI tracking detectors was $\Delta(1/p_t) = 0.0008(\mathrm{GeV/c})^{-1}$ for particles (except electrons) with the same momentum as the beam. Calibration of the momentum is performed with $e^+e^- \to \mu^+\mu^-$ events. For lower momenta the masses of the K^0_s and the J/ψ are reconstructed to give an absolute momentum scale for particles other than electrons estimated, to a precision of 0.2% over the full momentum range.

The determination of the momentum of electrons is somewhat more complicated. In passing through the RICH from the TPC to the OD, particles traverse about 60% of a radiation length. A large fraction of electrons therefore lose a substantial amount of energy through bremsstrahlung before they reach the OD. Due to this the standard momentum measurement of electrons would always tend to be biased to lower values. This effect is somewhat reduced through only using the measured momentum without using the OD, p'. The result is that this "refit momentum" shows a more Gaussian behaviour than the standard momentum fit. The best estimate for the momentum of the electron, p_{el}, is constructed in such a way as to benefit from the better resolution of the momentum measurement at low momentum and the smaller bremsstrahlung bias of the electromagnetic energy measurement. The reconstructed track momentum and

the electromagnetic energy were combined through a weighted average which took into account the downward biases of the two respective measurements. The energy of the radiated photons was also added to the electromagnetic energy measurement to reduce the effects of bremsstrahlung further.

An algorithm was used which performed a weighted average depending on the value of E_{ass}/p'. The further this value was from unity, the more the weight of the estimator with the lower value was down scaled relative to the other. The scaling factor was inversely proportional to the square of the number of standard deviations by which the value of E_{ass}/p' was from unity.

Subsequent references to the momenta of electrons imply the use of the best estimator p_{el}. The momenta of other particles are measured using the standard momentum fit, p, of the particle as it traverses the detector.

6 The selection of the event sample

In order to determine the Michel parameters, a sample of exclusively selected leptonic decays of the τ together with an inclusive sample of semi-leptonic decays have been used. The data sample corresponds to the data taken by DELPHI during 1992 (22.9 pb^{-1} at $E_{cm} = 91.3$ GeV), 1993 (15.7 pb^{-1} at $E_{cm} = 91.2$ GeV, 9.4 pb^{-1} at $E_{cm} = 89.2$ GeV and 4.5 pb^{-1} at $E_{cm} = 93.2$ GeV), 1994 (47.4 pb^{-1} at $E_{cm} = 91.2$ GeV) and 1995 (14.3 pb^{-1} at $E_{cm} = 91.2$ GeV, 9.2 pb^{-1} at $E_{cm} = 89.2$ GeV and 9.3 pb^{-1} at $E_{cm} = 93.2$ GeV).

In all analyses, samples of simulated events were used which had been passed through a detailed simulation of the detector response [23] and reconstructed with the same program as the real data. The Monte Carlo event generators used were: KORALZ [24] for $e^+e^- \to \tau^+\tau^-$ events; DYMU3 [25] for $e^+e^- \to \mu^+\mu^-$ events; BABAMC [26] for $e^+e^- \to e^+e^-$ events; JETSET 7.3 [27] for $e^+e^- \to q\overline{q}$ events; Berends-Daverveldt-Kleiss [28] for $e^+e^- \to e^+e^-e^+e^-$, $e^+e^- \to e^+e^-\mu^+\mu^-$ and $e^+e^- \to e^+e^-\tau^+\tau^-$ events.

The selection is described in detail in [29]. The variables used in the initial preselection of the τ sample together with the selection of the various decay channels are briefly described below.

6.1 The $e^+e^- \to \tau^+\tau^-$ sample

At LEP energies, a $\tau^+\tau^-$ event appears as two highly collimated low multiplicity jets in approximately opposite directions. An event was separated into hemispheres by a plane perpendicular to the event thrust axis, where the thrust was calculated using all charged particles. To be included in the sample, it was required that the highest momentum charged particle in at least one of the two hemispheres lie in the polar angle range $|cos\Theta| < 0.732$.

Background from $e^+e^- \to q\overline{q}$ events was reduced by requiring a charged particle multiplicity less than six and a minimum thrust value of 0.996. The $e^+e^- \to q\overline{q}$ background is however a negligible background in the analysis of the Michel parameters as one is looking for events with only one charged track in each hemisphere.

Cosmic rays and beam gas interactions were rejected by requiring that the highest momentum charged particle in each hemisphere have a point of closest approach to the interaction region less than 4.5 cm in z and less than 1.5 cm in the $r - \phi$ plane. It

was furthermore required that these particles have a difference in z of their points of closest approach at the interaction region of less than 3 cm. The offset in z of tracks in opposite hemispheres of the TPC was sensitive to the time of passage of a cosmic ray event with respect to the interaction time of the beams. The background left in the selected sample was computed from the data by interpolating the distributions outside the selected regions.

Two-photon events were removed by requiring a total energy in the event greater than 8 GeV and a total event transverse momentum greater than 0.4 GeV/c.

Contamination from $e^+e^- \to e^+e^-$ and $e^+e^- \to \mu^+\mu^-$ events was reduced by requiring that the event acollinearity, $\theta_{acol} = cos^{-1}(-\frac{p_1 \cdot p_2}{|p_1||p_2|})$, be greater than 0.5°. The variables P_1 and P_2 are the momenta of the highest momenta charged particles in hemisphere 1 and 2 respectively.

The $e^+e^- \to e^+e^-$ background is reduced in the second instance with a cut on the radial energy E_{rad} (defined as $E_{rad} = \sqrt{{E_1}^2 + {E_2}^2}/E_{beam}$ where E_1 and E_2 are the energies deposited in the HPC in a 30° cone around the highest momentum charged particle in each hemisphere and E_{beam} is the beam energy). Events are retained if $E_{rad} < 1$.

The $e^+e^- \to \mu^+\mu^-$ background is reduced in the second instance with a cut on the radial momentum P_{rad} (defined as $P_{rad} = \sqrt{{P_1}^2 + {P_2}^2}/P_{beam}$ where P_1 and P_2 are the momenta of the highest momentum charged particles in each hemisphere and P_{beam} is the beam momentum). Cutting on this quantity is also effective in reducing the $e^+e^- \to e^+e^-$ background. Events are retained if $P_{rad} < 1$.

As a result of the above selection ~ 93000 $e^+e^- \to \tau^+\tau^-$ candidates were selected from the 1992 to 1995 data set. The efficiency of selection in the 4π solid angle was $\sim 54\%$. The background arising from $e^+e^- \to e^+e^-$ events was estimated to be $(1.07 \pm 0.32)\%$, from $e^+e^- \to \mu^+\mu^-$ events $(0.30 \pm 0.09)\%$ and from four-fermion processes $(0.93 \pm 0.28)\%$. The efficiencies and backgrounds varied slightly from year to year, the data sets were therefore treated independently.

6.2 The $\tau \to e\overline{\nu}_e\nu_\tau$ channel

The $\tau \to e\overline{\nu}_e\nu_\tau$ decay has the signature of an isolated charged particle which produces an electromagnetic shower in the calorimetry. The produced electrons are ultra-relativistic and leave an ionisation deposition in the Time Projection Chamber corresponding to the plateau region above the relativistic rise. Backgrounds from other τ decays arise principally from one-prong hadronic decays where either the hadron interacts early in the electromagnetic calorimetry or an accompanying π^0 decay is wrongly associated to the charged particle track.

To identify an electron it was required that there be one charged particle in the hemisphere with a momentum greater than $0.01p_{beam}$. To ensure optimal use of the HPC it was required that the track lie in the polar angle range $0.035 < |cos\Theta| < 0.707$ and that the track extrapolation to the HPC should lie outside any HPC azimuthal boundary region, as described in Section 4.

The dE/dx measurement is crucial to the analysis and so it was required that there were at least 28 anode wires with ionisation information in the TPC. It was required that the dE/dx measurement be consistent with that of an electron by requiring that the $\prod^e_{dE/dx}$ variable be greater than -2. This requirement was efficient, especially at low momentum, in retaining signal and removing backgrounds from muons and hadrons.

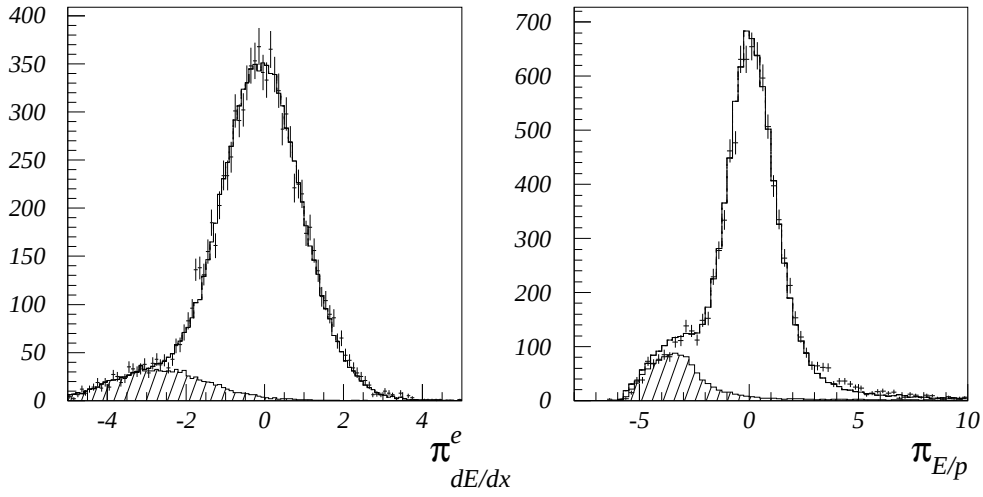

Figure 3: The $\prod^e_{dE/dx}$ and $\prod_{E/p}$ variables after application of all the other selection cuts except the one shown for 1994 data. The points are the real data, the solid histogram is the sum of the signal and background and the shaded area is the background from $\tau \not\to e\nu\overline{\nu}$ events.

Background was reduced still further with a logical "OR" of two selections, the first on the $\prod^{\pi}_{dE/dx}$ variable, which was particularly good at low momentum, and the second on the $\prod_{E/p}$ variable, which was particularly good at high momentum. The "OR" thus gives a high constant efficiency over the whole momentum range. The $\prod^e_{dE/dx}$ and $\prod_{E/p}$ variables can be seen in figure 3.

To reduce the remaining background further it was required that there be no hits in the muon chambers and no deposited energy beyond the first HCAL layer. Residual background from $\tau \to \pi(n\pi^0)\nu$ was reduced by cutting on the energy of the most energetic neutral shower in the HPC observed in an 18° cone around the track. Neutral showers were not included in this requirement if they were within 1° of the track and hence compatible with being bremsstrahlung photons.

The identification criteria were studied on test samples of real data. The efficiency of the dE/dx and HPC cuts were tested across the whole momentum range by exploiting the redundancy of the two. Since the simulation showed that the two measurements were instrumentally uncorrelated, the overall bin by bin efficiency was calculated from these two independent measurements.

Backgrounds arising from non-τ sources consisted of $e^+e^- \to e^+e^-$ and four-fermion $e^+e^- \to e^+e^-e^+e^-$ events. The $e^+e^- \to e^+e^-$ background was suppressed by the standard τ preselection cuts, *i.e.* $P_{rad} < 1$ and $E_{rad} < 1$. Four-fermion events remaining after the E_{vis} and P_t^{miss} cuts were further suppressed by demanding that if the $\tau \to e\nu\overline{\nu}$ candidate had a momentum less than $0.2E_{beam}$ and there was only one particle with a momentum below $0.2E_{beam}$ in the other hemisphere then this particle was required to have $\prod^{\pi}_{dE/dx} > 3$; otherwise the event was rejected.

As a result of the above procedure ~ 21500 $\tau \to e\overline{\nu}_e\nu_\tau$ candidates were selected from the 1992 to 1995 data. The efficiency of selection within the 4π angular acceptance was 35%. The background arising from $\tau \not\to e\overline{\nu}_e\nu_\tau$ processes was estimated to be $(3.89 \pm 1.17)\%$, from $e^+e^- \to e^+e^-$ events $(1.61 \pm 0.48)\%$ and from $e^+e^- \to e^+e^-e^+e^-$ events

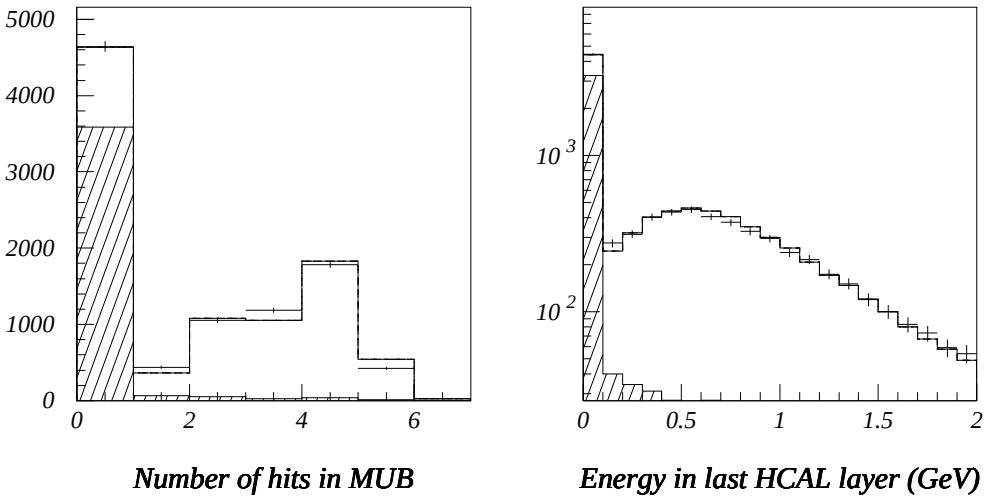

Figure 4: The number of hits in the muon chambers and the energy deposited in the last layer of the HCAL after application of all the other selection cuts except the one shown for 1993 data. The points are the real data, the solid histogram is the sum of the signal and background and the shaded area is the background from $\tau \not\to \mu\nu\overline{\nu}$ events.

$(0.53 \pm 0.16)\%$.

6.3 The $\tau \to \mu\overline{\nu}_\mu\nu_\tau$ channel

A muon candidate in the decay $\tau \to \mu\overline{\nu}_\mu\nu_\tau$ appears as a minimum ionising particle in the hadron calorimeter, penetrating through to the muon chambers. Due to ionisation loss, a minimum momentum of about 2 GeV/c is required for a muon to pass through the hadron calorimeter.

To identify a muon it was required that there be one charged particle in the hemisphere with sufficient energy to penetrate through the detector into the muon chambers. Thus the candidate had to have a momentum greater than $0.05p_{beam}$ and lie within the polar angle interval $0.035 < |cos\Theta| < 0.732$.

To be identified positively as a muon it was required that the track deposited energy deep in the HCAL or have a hit in the muon chambers. This was achieved specifically in the first instance by insisting that the average energy per HCAL layer E_{hlay} be less than 2 GeV. The logical "OR" of two variables was also used in the selection. The track was required to either have a maximum deposited energy in any HCAL layer of less than 3 GeV together with deposited energy greater than 0.2 GeV in the last HCAL layer, or have at least one hit in the muon chambers. This combination of cuts gave a reasonably constant efficiency over the whole momentum range. The two selection variables, the energy deposited in the last HCAL layer and the number of hits in the muon chambers, can be seen in figure 4.

To suppress background further it was required that the sum of the energies of all the electromagnetic neutral showers in an 18° cone around the track did not exceed 2 GeV. This cut was effective in further suppressing $\tau \to \pi(n\pi^0)$ and $e^+e^- \to \mu^+\mu^-\gamma$ events.

The identification criteria were studied on test samples of real data. The efficiencies of the HCAL and muon chamber cuts were tested across the whole momentum range

by exploiting the redundancy of the two. The simulation was found to model the data sufficiently well.

Backgrounds arising from non-τ sources consisted mainly of $e^+e^- \to \mu^+\mu^-$, $e^+e^- \to e^+e^-\mu^+\mu^-$, $e^+e^- \to e^+e^-\tau^+\tau^-$ and cosmic events. The $e^+e^- \to \mu^+\mu^-$ background was suppressed by the standard preselection cut, i.e. $P_{rad} < 1$. The remaining background was further suppressed by demanding that the event was rejected if there was an identified muon in each hemisphere with momentum greater than $0.8E_{beam}$ and the total visible energy was greater than 70% of the centre-of-mass energy. The event was also rejected if the momentum of the identified muon was greater than $0.8p_{beam}$ and the momentum of the leading track in the opposite hemisphere was greater than $0.8p_{beam}$.

The four-fermion events $e^+e^- \to e^+e^-\mu^+\mu^-$ and $e^+e^- \to e^+e^-\tau^+\tau^-$, although background processes, required no further suppression.

Also used in this analysis was a selected sample of $\tau \to \mu\overline{\nu}_\mu\nu_\tau$ candidates with momenta below 2 GeV. At these energies muons do not have sufficient energy to penetrate through the HCAL to reach the muon chambers, thus making the selection more difficult. Instead, at these lower momenta, muon candidates were selected if the particle was seen in the last 3 layers of the HCAL. This procedure was tested using a sample of hadrons selected from the data and Monte Carlo by tagging ρ decays through the presence of a π^0 in the HPC. In order to study the signal, various variables were compared in the data and Monte Carlo to see if the simulation correctly modelled the performance of DELPHI at these low energies. The response of the HCAL to these hadrons and muons with momenta below 2 GeV was well described by the simulation.

As a result of the above procedure ~ 26500 $\tau \to \mu\overline{\nu}_\mu\nu_\tau$ candidates were selected from the 1992 to 1995 data. The efficiency of selection within the 4π angular acceptance was 48%, the background arising from $\tau \not\to \mu\overline{\nu}_\mu\nu_\tau$ processes was estimated to be (1.88 ± 0.56)%, from $e^+e^- \to \mu^+\mu^-$ events (0.52 ± 0.16)%, from $e^+e^- \to e^+e^-\mu^+\mu^-$ events (0.58 ± 0.17)%, from $e^+e^- \to e^+e^-\tau^+\tau^-$ events (0.48 ± 0.14)% and from cosmics (0.14 ± 0.04)%.

6.4 The $\tau \to h(n\pi^0)\nu_\tau$ channel

The $\tau \to$ inclusive one-prong hadrons channel makes no distinction between the primary semi-leptonic decays namely $\tau \to \pi\nu_\tau$, $\tau \to \rho\nu_\tau$ and $\tau \to a_1\nu_\tau$. Instead each decay candidate is separated into bins of invariant mass, constructed from the 4-momenta of the charged particles and all reconstructed photons. The invariant mass bins used were $M_{inv} < 0.3$ GeV, 0.3 GeV $< M_{inv} <$ 0.95 GeV and $M_{inv} >$ 0.95 GeV.

The preselection of the τ's for this channel is slightly different to that for the leptonic channels due to the smaller potential backgrounds arising from di-lepton events. Therefore the preselection cuts are loosened somewhat and, specifically, the P_{rad} cut is not used and the E_{rad} cut is loosened to 1.1.

To identify hadrons one is forced to use almost all the components of the detector. To be identified as a hadron it is required that only the leading particle in the hemisphere has associated vertex detector hits (to retain a high efficiency in picking up events with conversions) and that the track lie within the barrel region, *i.e.* $0.035 < |cos\Theta| < 0.732$.

Further cuts were made depending on the invariant mass of the decay products. Figure 5 shows the invariant mass distribution for all preselected τ's, calculated assuming that all charged particles were pions and all neutral tracks were photons. One can see that most background from leptons comes at low invariant mass. Hence one should apply

stricter criteria for these events.

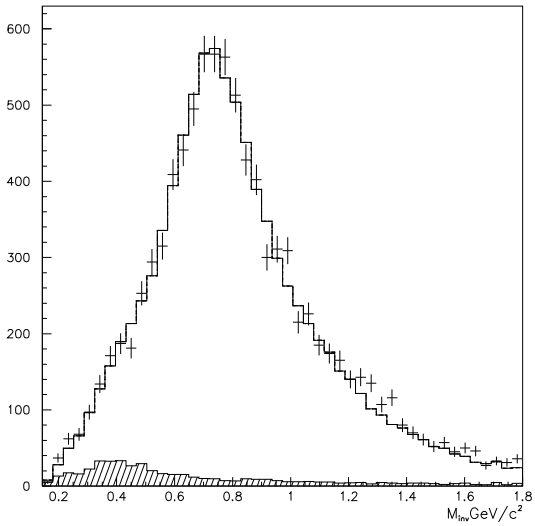

Figure 5: The invariant mass distribution for all preselected τ decays in 1995 data. The points are the real data, the solid histogram is the simulated $e^+e^- \rightarrow \tau^+\tau^-$ data together with the simulated background, the shaded area is the sum of the $e^+e^- \rightarrow e^+e^-$, $e^+e^- \rightarrow \mu^+\mu^-$ and the leptonic τ decays. The pole at the $\pi^\pm$ mass is not plotted.

The background from electrons was suppressed with the following two cuts. Firstly the measured dE/dx in the TPC had to be consistent with being a pion, so $\prod^{\pi}{}_{dE/dx} < 2$. Because of the importance of the dE/dx measurement to the selection it was also required that there were at least 28 anode wires with an ionisation measurement. This cut is particularly effective at low momentum.

The second cut required that either the particle deposited an energy beyond the first layer of the HCAL or that the associated energy in the first four layers of the HPC be less than 1 GeV for invariant masses below 0.3 GeV, and 5 GeV otherwise. This cut is particularly effective at high momentum. The combination of the two cuts therefore leads to an even efficiency for the suppression of electrons across the whole momentum range.

Rejection of background from muons was only performed for events with invariant masses less than 0.3 GeV. Muon background in higher invariant mass bins was found to be small enough to justify no further suppression. The muon rejection was based on the average energy per HCAL layer, E_{hlay}. It was required that this was either zero or greater than 2 GeV. In addition to this criteria it was also required that there were no hits in the muon chambers and that the momentum of the leading charged particle was greater than $0.05p_{beam}$ in order that the it had sufficient energy to reach the muon chambers. For regions not covered by the muon chambers it was required that there was no deposition in the last two layers of the HCAL. In this instance any tracks pointing to HCAL azimuthal boundaries were rejected.

The identification criteria were studied with test samples of real data. The efficiencies of all the main selection cuts were tested using a sample of hadrons selected by tagging π^0's in the HPC. This test sample allowed for an accurate calibration of all the main selection variables across the whole range of $cos\theta^*$ and $cos\psi$, the two variables used in the fits to the Michel parameters and the anomalous tensor coupling.

Remaining background from $e^+e^- \to e^+e^-$ and $e^+e^- \to \mu^+\mu^-$ events was suppressed by demanding that the particle in the opposite hemisphere to the identified hadron had a measured momentum of less than $0.8p_{beam}$. The four-fermion events $e^+e^- \to e^+e^-\tau^+\tau^-$ required no further suppression.

As a result of the above procedure $\sim$ 56000 $\tau \to h(n\pi^0)\nu_\tau$ candidates were selected from the data. The efficiency of selection within the 4π angular acceptance was 37%, the background arising from $\tau \not\to h(n\pi^0)\nu_\tau$ processes was estimated to be $(2.43 \pm 0.73)\%$ from $e^+e^- \to e^+e^-$ events, $(0.40 \pm 0.12)\%$ from $e^+e^- \to \mu^+\mu^-$ events $(0.10 \pm 0.03)\%$ and from $e^+e^- \to e^+e^-\tau^+\tau^-$ events $(0.23 \pm 0.07)\%$.

6.5 The two-dimensional selection

As has already been described, in order to measure the Michel parameters most efficiently it is necessary to use two-dimensional spectra. It was required that the events satisfied the preselection cuts and that there was one identified candidate τ decay in each hemisphere. This therefore produces 20 (15 two-dimensional and 5 one-dimensional) distributions consisting of $e\mu$, ee, $\mu\mu$, $eh1$,[1] $eh2$, $eh3$, $\mu h1$, $\mu h2$, $\mu h3$, $h1h1$, $h2h2$, $h3h3$, $h1h2$, $h1h3$, $h2h3$, eX, μX, $h1X$, $h2X$ and $h3X$, where the two identified particles in each correspond to the two hemispheres in the event. The X in the event is an unidentified τ decay with either one or three charged particles. In this case only the hemisphere with the identified track is used.

In most of these channels it is required that the τ preselection cuts be satisfied in order that non-τ backgrounds be suppressed. This is not true for the $e\mu$ channel in which no preselection cuts were necessary as the external background required no further suppression. To suppress remaining cosmic background in the $\mu\mu$ and the μX samples it was required, in one-versus-one charged particle topologies, that at least one of the charged particle tracks extrapolated to within 0.3 cm in the $r-\phi$ plane of the interaction region. For the one dimensional distributions, eX, μX, $h1X$, $h2X$ and $h3X$, the cuts to remove external backgrounds follow those already outlined in the previous sections describing the one dimensional selections.

The number of events selected, the efficiency of selection within the fiducial volume and momentum acceptance and the backgrounds can be seen in tables 1 and 2.

7 The extraction of the Michel parameters

The values of the Michel parameters, ρ, η, ξ and $\xi\delta$ together with the tau polarisation, $\mathcal{P}_\tau$, and the tau neutrino helicity, h_{ν_τ}, are extracted from the data using a binned maximum likelihood fit to all the combinations of $\tau \to e\overline{\nu}_e\nu_\tau$, $\tau \to \mu\overline{\nu}_\mu\nu_\tau$ and $\tau \to h(n\pi^0)\nu_\tau$. In splitting the hadron sample into 3 invariant mass bins one is left with 15 two-dimensional and 5 one-dimensional distributions where only one τ decay has been exclusively identified.

The likelihood function is defined as:

$$\mathcal{L} = \prod_i \prod_j \frac{{\nu_{ij}}^{n_{ij}}\, e^{-\nu_{ij}}}{n_{ij}!} \tag{24}$$

[1] where h1,h2 and h3 are hadrons in the invariant mass bins $M_{inv} < 0.3\ GeV/c^2$, $0.3\ GeV/c^2 < M_{inv} < 0.95\ GeV/c^2$ and $M_{inv} > 0.95\ GeV/c^2$ respectively

channel	efficiency(%)
$Z^0 \to \tau^+\tau^- \to (e\nu\overline{\nu})(\mu\nu\overline{\nu})$	72.95 ± 0.23
$Z^0 \to \tau^+\tau^- \to (e\nu\overline{\nu})(e\nu\overline{\nu})$	50.43 ± 0.36
$Z^0 \to \tau^+\tau^- \to (\mu\nu\overline{\nu})(\mu\nu\overline{\nu})$	82.77 ± 0.27
$Z^0 \to \tau^+\tau^- \to (e\nu\overline{\nu})(h(n\pi^0)\nu)$	47.08 ± 0.15
$Z^0 \to \tau^+\tau^- \to (\mu\nu\overline{\nu})(h(n\pi^0)\nu)$	60.23 ± 0.15
$Z^0 \to \tau^+\tau^- \to (h(n\pi^0)\nu)(h(n\pi^0)\nu)$	37.62 ± 0.13

Table 1: The efficiencies of selection in the angular and momentum acceptance for the two dimensional analysis in the 1994 data set. The efficiencies were of a similar magnitude for the other years. The errors are purely statistical.

channel	no. of candidates	internal background (%)	external background(%)
$e\mu$	3495	4.43 ± 1.33	0.60 ± 0.18
ee	1405	6.01 ± 1.80	7.19 ± 2.16
$\mu\mu$	2116	2.61 ± 0.78	3.89 ± 1.17
$eh2$	3324	3.92 ± 1.18	0.11 ± 0.03
$\mu h2$	4454	2.13 ± 0.64	0.54 ± 0.16
$h2h2$	2295	1.69 ± 0.51	0.12 ± 0.04
$h1h2$	2271	3.19 ± 0.96	0.10 ± 0.03
$eh1$	1804	5.31 ± 1.59	0.60 ± 0.18
$\mu h1$	2160	3.88 ± 1.16	0.30 ± 0.09
$eh3$	1088	4.01 ± 1.20	0.21 ± 0.06
$\mu h3$	1480	2.09 ± 0.63	0.80 ± 0.24
$h1h3$	730	3.12 ± 0.94	0.15 ± 0.05
$h2h3$	784	1.80 ± 0.54	0.01 ± 0.01
$h1h1$	571	4.89 ± 1.47	0.20 ± 0.06
$h3h3$	278	1.93 ± 0.58	0.01 ± 0.01
eX	6377	2.96 ± 0.89	4.66 ± 1.40
μX	8632	1.58 ± 0.47	1.36 ± 0.41
$h1X$	5104	2.54 ± 0.76	1.87 ± 0.56
$h2X$	9342	0.93 ± 0.28	0.33 ± 0.10
$h3X$	3058	0.94 ± 0.28	0.16 ± 0.05

Table 2: The number of events and backgrounds for the two dimensional selection. The backgrounds are quoted for the 1994 data set only. They were of a similar magnitude for the other years. A total of 60768 events were selected in the 1992-1995 sample.

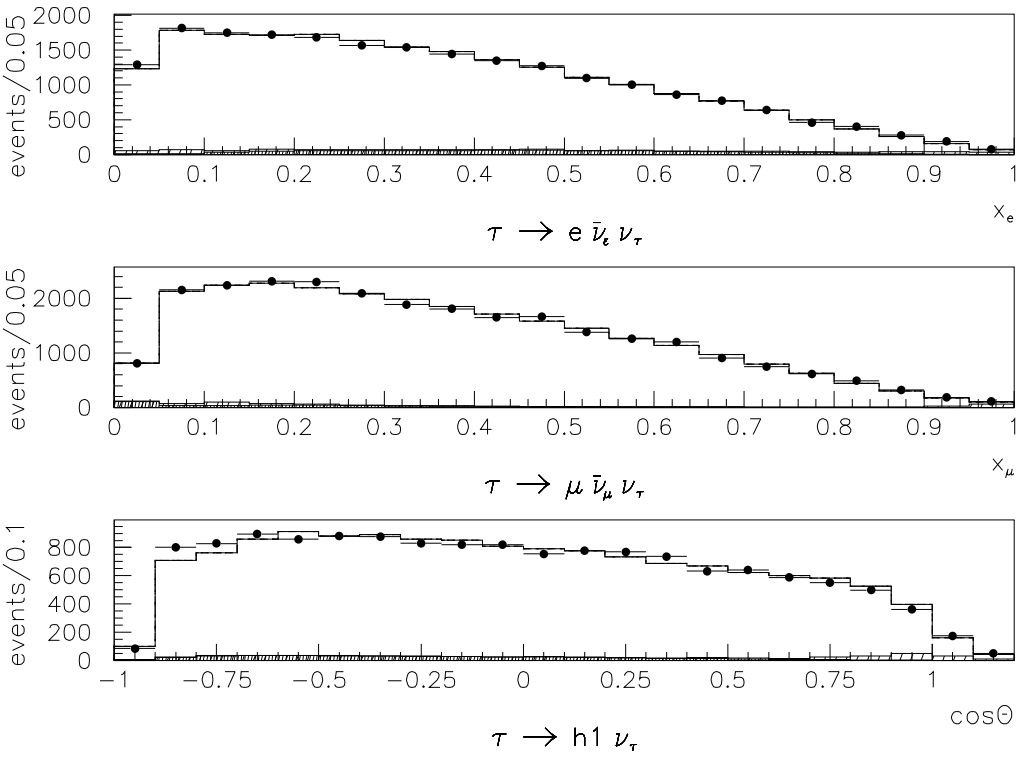

Figure 6: The fitted distributions for the six parameter fit for the two fully leptonic decay channels and the semi-leptonic candidates from the lowest invariant mass bin. The line is the result of the fit, the points are the data, the light shading is the sum of all backgrounds and the darker shading is the internal background.

where i denotes the particular form of decays used and j denotes the bins of the fit. n_{ij} and ν_{ij} denote respectively the number in the data and the expected number of events for the case i. The choice of normalisation was as follows. The non-τ background was normalised to the luminosity of the data. The τ internal background was normalised such that the fraction of τ background in the fit was the same as seen in the Monte Carlo. The signal was normalised so that the total number of events seen in the real data was the same as predicted by the corrected theoretical distributions.

In the case of leptonic decays of the τ the expected number ν_{ij} is obtained using the KORALZ [24] Monte Carlo generator together with a modified version of the TAUOLA [30] package which allows the setting of different non-Standard Model values for the Michel parameters. The distributions are constructed by generating large samples of decays with different Michel parameters. These samples are then used to form the polynomials of the decay. In order to obtain distributions which can be directly fitted to the data it was then necessary to correct the generator level information for effects of resolution and efficiency within the DELPHI detector. This was achieved using the full detector simulation.

For the semi-leptonic decays of the τ the distributions used in the fit were obtained from fully simulated Monte Carlo events. The polynomials were constructed using the positive and negative helicity states of the decaying τ to give a distribution which could be used directly in the fit.

Under the assumption of lepton universality the value of η_l can be constrained in the

fit to that from the measured values of the leptonic branching ratios using equation 4. The branching ratio results used were those from the same data set as used to measure the Michel parameters [31]. The value of η_l was constrained with the addition of the following factor on to the likelihood function

$$ln\mathcal{L}^{\text{const}} = -\frac{1}{2}\frac{(\eta_l - \eta_{Br})^2}{\Delta\eta_{Br}^2}, \tag{25}$$

where η_l is the fitted value, η_{Br} is the value obtained from the leptonic branching ratio measurement and $\Delta\eta_{Br}$ is the error on this measurement.

It must however be noted that obtaining the equation 4 involves an integration over the final state momenta, the implications of which have to be accounted for when setting a limit on η based on experimentally measured branching fractions. Since η affects the shape of the muon momentum spectrum as well as the total decay rate, it is necessary to study the effect of the cutoff on the muon momentum identification which is at $x^c = p^c/p_{beam} = 0.05$. As a function of the normalized laboratory muon momentum $x = p/p_{beam}$ the number of events observed between momentum x and $x + dx$ can be written as

$$dN = N_0\left[a(x) + K\eta b(x)\right]dx. \tag{26}$$

The polynomials $a(x), b(x)$ are functions of the readily obtainable decay distribution expressed in the τ rest frame as a function of energy, decay angle, τ polarisation and the other Michel parameters, with well defined values in the Standard Model [15, 14]. The constants N_0 and K can always be chosen such that the integrals of $a(x)$ and $b(x)$ over the whole momentum range are normalized to 1. If η is non-zero, the number of events observed would be

$$N_{obs} = N_0\left[\int_{x^c}^{x^{max}} a(x)dx + K\eta\int_{x^c}^{x^{max}} b(x)dx\right]. \tag{27}$$

The event generator used to compute acceptance corrections assumes that η equals zero. In other words, the branching ratio is derived assuming that the total number of $\tau \to \mu$ decays produced can be estimated as

$$N_0^{est} = N_{obs} \times \frac{1}{\int_{x^c}^{x^{max}} a(x)dx} \tag{28}$$

where the integral is obtained from simulation. Hence, instead of correcting to obtain $N_0^{est} = N_0 + K\eta$, the estimate of the corrected number of events becomes

$$N_0^{est} = N_0\left[1 + K\eta\frac{\int_{x^c}^{x^{max}} b(x)dx}{\int_{x^c}^{x^{max}} a(x)dx}\right]. \tag{29}$$

The ratio between the integrals is readily calculated numerically by generating the full distribution in the τ rest frame and boosting the momentum to the lab frame. It is found that the ratio between the integrals equals 0.96 when integrating from $x^c = 0.05$. Ignoring effects due to η in $\tau \to e$ decays, the relation

$$\frac{Br(\tau \to \mu\nu_\tau\overline{\nu}_\mu)}{Br(\tau \to e\nu_\tau\overline{\nu}_e)} = f\left(\frac{m_\mu^2}{m_\tau^2}\right) + 3.84\frac{m_\mu}{m_\tau}g\left(\frac{m_\mu^2}{m_\tau^2}\right)\eta. \tag{30}$$

should be used to extract η from the DELPHI tau leptonic branching ratios instead of equation (4).

Using the techniques outlined above together with background distributions obtained from the Monte Carlo simulation a six parameter and a nine parameter fit were performed, with and without the assumption of lepton universality respectively, over a sample of $\sim$60000 τ pair candidates (see figures 6 and 7). The systematics on the measurement arose from the finite amount of Monte Carlo data available; the uncertainties in the world average values of the τ branching ratios; the uncertainties in the levels of the backgrounds; uncertainties in the efficiency of selection and finally calibration uncertainties on the selection and fit variables. For the particular case of the fit assuming lepton universality there is an additional systematic arising from the uncertainties on the leptonic branching ratio measurement. The systematics are summarised in tables 3 and 4.

	η_l	ρ_l	$\mathcal{P}_\tau$	ξ_l	$\xi_l\delta_l$	h_{ν_τ}
MC stats	0.0053	0.0035	0.0018	0.0104	0.0103	0.0039
τ BR's	0.0002	0.0006	0.0014	0.0004	0.0012	0.0020
Backgrounds	0.0251	0.0115	0.0011	0.0030	0.0126	0.0093
Efficiency	0.0005	0.0023	0.0037	0.0013	0.0027	0.0014
Calibration	0.0144	0.0146	0.0065	0.0281	0.0229	0.0034
η_l const.	0.0232	0.0070	-	-	-	-
Total	0.037	0.020	0.008	0.030	0.028	0.011
Statistical	0.036	0.023	0.012	0.070	0.070	0.027

Table 3: The systematics on the parameters for the six parameter fit with the assumption of universality. The statistical error is shown for comparison.

	η_μ	ρ_e	ρ_μ	$\mathcal{P}_\tau$	ξ_e	ξ_μ	$\xi_e\delta_e$	$\xi_\mu\delta_\mu$	h_{ν_τ}
MC stats	0.047	0.0054	0.0144	0.0018	0.0177	0.028	0.019	0.019	0.0039
τ BR's	0.003	0.0008	0.0016	0.0016	0.0017	0.001	0.001	0.001	0.0003
Backgrounds	0.138	0.0230	0.0414	0.0060	0.0058	0.044	0.018	0.018	0.0093
Efficiency	0.010	0.0034	0.0017	0.0036	0.0020	0.003	0.001	0.001	0.0014
Calibration	0.039	0.0278	0.0076	0.0069	0.0438	0.018	0.034	0.033	0.0045
Total	0.15	0.037	0.045	0.010	0.05	0.06	0.04	0.04	0.011
Statistical	0.32	0.036	0.098	0.012	0.12	0.19	0.12	0.13	0.028

Table 4: The systematics on the parameters for the nine parameter fit without the assumption of universality. The statistical error is shown for comparison.

The six parameter fit assuming lepton universality (including the constraint on η from the leptonic branching ratios) gave the following results:

$$\begin{aligned} \eta_l &= -0.005 \pm 0.036 \pm 0.037, \\ \rho_l &= 0.775 \pm 0.023 \pm 0.020, \end{aligned}$$

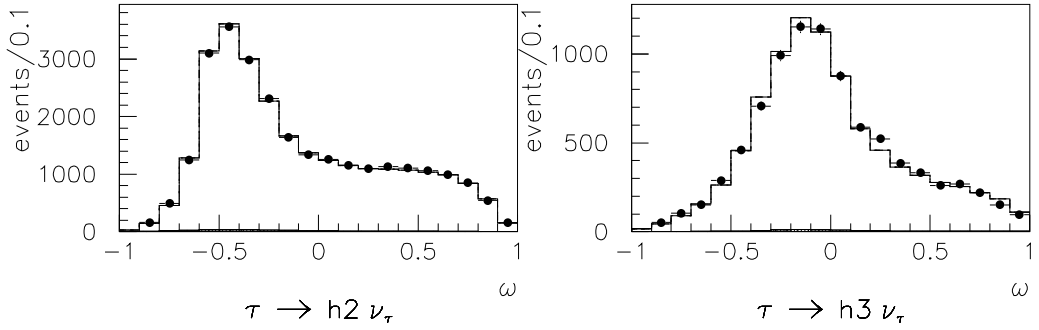

Figure 7: The fitted distributions for the six parameter fit for the semi-leptonic candidates selected in the second and third invariant mass bins. The line is the result of the fit, the points are the data, the light shading is the sum of all backgrounds and the darker shading is the internal background.

$$\begin{aligned} \xi_l &= 0.929 \pm 0.070 \pm 0.030, \\ \xi_l\delta_l &= 0.779 \pm 0.070 \pm 0.028, \\ h_{\nu_\tau} &= -0.997 \pm 0.027 \pm 0.011, \\ \mathcal{P}_\tau &= -0.130 \pm 0.012 \pm 0.008. \end{aligned}$$

The parameters are correlated and the correlation matrix is given in table 5.

	η_l	ρ_l	$\mathcal{P}_\tau$	ξ_l	$\xi_l\delta_l$	h_{ν_τ}
η_l	1.00	0.276	-0.016	0.100	0.070	0.009
ρ_l		1.00	0.435	-0.060	-0.105	-0.205
$\mathcal{P}_\tau$			1.00	0.040	-0.188	-0.414
ξ_l				1.00	-0.142	0.062
$\xi_l\delta_l$					1.00	0.190

Table 5: The correlation matrix for the six parameter fit.

Also measured was the variable P_R^τ, defined in equation 5, which represents the probability of a right handed τ decaying into a lepton of either handedness. This was measured to be

$$P_R^\tau = -0.038 \pm 0.066 \pm 0.029.$$

A one-dimensional fit to η_l was also performed. In setting the other Michel parameters to their Standard Model values and applying the branching ratio constraint (equation 30) the value of η_l was measured to be

$$\eta_l = -0.009 \pm 0.033 \pm 0.024.$$

The nine parameter fit without any assumption of universality gave the following results:

$$\begin{aligned}
\eta_\mu &= 0.72 \pm 0.32 \pm 0.15, \\
\rho_e &= 0.744 \pm 0.036 \pm 0.037, \\
\rho_\mu &= 0.999 \pm 0.098 \pm 0.045, \\
\xi_e &= 1.01 \pm 0.12 \pm 0.05, \\
\xi_\mu &= 1.16 \pm 0.19 \pm 0.06, \\
\xi_e\delta_e &= 0.85 \pm 0.12 \pm 0.04, \\
\xi_\mu\delta_\mu &= 0.86 \pm 0.13 \pm 0.04, \\
h_{\nu_\tau} &= -0.991 \pm 0.028 \pm 0.014, \\
\mathcal{P}_\tau &= -0.131 \pm 0.012 \pm 0.011.
\end{aligned}$$

The parameters are correlated and the correlation matrix is given in table 6.

	η_μ	ρ_e	ρ_μ	$\mathcal{P}_\tau$	ξ_e	ξ_μ	$\xi_e\delta_e$	$\xi_\mu\delta_\mu$	h_{ν_τ}
η_μ	1.00	-0.102	0.937	-0.065	-0.003	0.678	-0.029	0.423	0.060
ρ_e		1.00	-0.071	0.331	-0.306	0.047	-0.230	0.032	-0.155
ρ_μ			1.00	0.062	0.059	0.569	0.012	0.327	-0.006
$\mathcal{P}_\tau$				1.00	-0.002	-0.035	-0.110	-0.130	-0.420
ξ_e					1.00	-0.184	0.342	-0.306	0.039
ξ_μ						1.00	-0.318	0.415	0.095
$\xi_e\delta_e$							1.00	-0.102	0.087
$\xi_\mu\delta_\mu$								1.00	0.157

Table 6: The correlation matrix for the nine parameter fit.

The values of the Michel parameters for the process $\tau \to \mu\overline{\nu}_\mu\nu_\tau$ are less precisely known than those from the $\tau \to e\overline{\nu}_e\nu_\tau$ channel. This is because for the $\tau \to \mu\overline{\nu}_\mu\nu_\tau$ channel one is also measuring the η parameter which has all its sensitivity in this channel. One can also see that the η_μ and ρ_μ parameters are both at the level of $\sim 2\sigma$ away from the Standard Model predictions. From the correlation matrix it is clear that these two parameters are highly correlated. In setting η_μ to its Standard Model prediction value of 0 one obtains the following results:

$$\begin{aligned}
\eta_\mu &= 0, \\
\rho_e &= 0.755 \pm 0.036 \pm 0.037, \\
\rho_\mu &= 0.789 \pm 0.028 \pm 0.012, \\
\xi_e &= 1.00 \pm 0.12 \pm 0.05, \\
\xi_\mu &= 0.87 \pm 0.11 \pm 0.03, \\
\xi_e\delta_e &= 0.86 \pm 0.12 \pm 0.04, \\
\xi_\mu\delta_\mu &= 0.733 \pm 0.094 \pm 0.030,
\end{aligned}$$

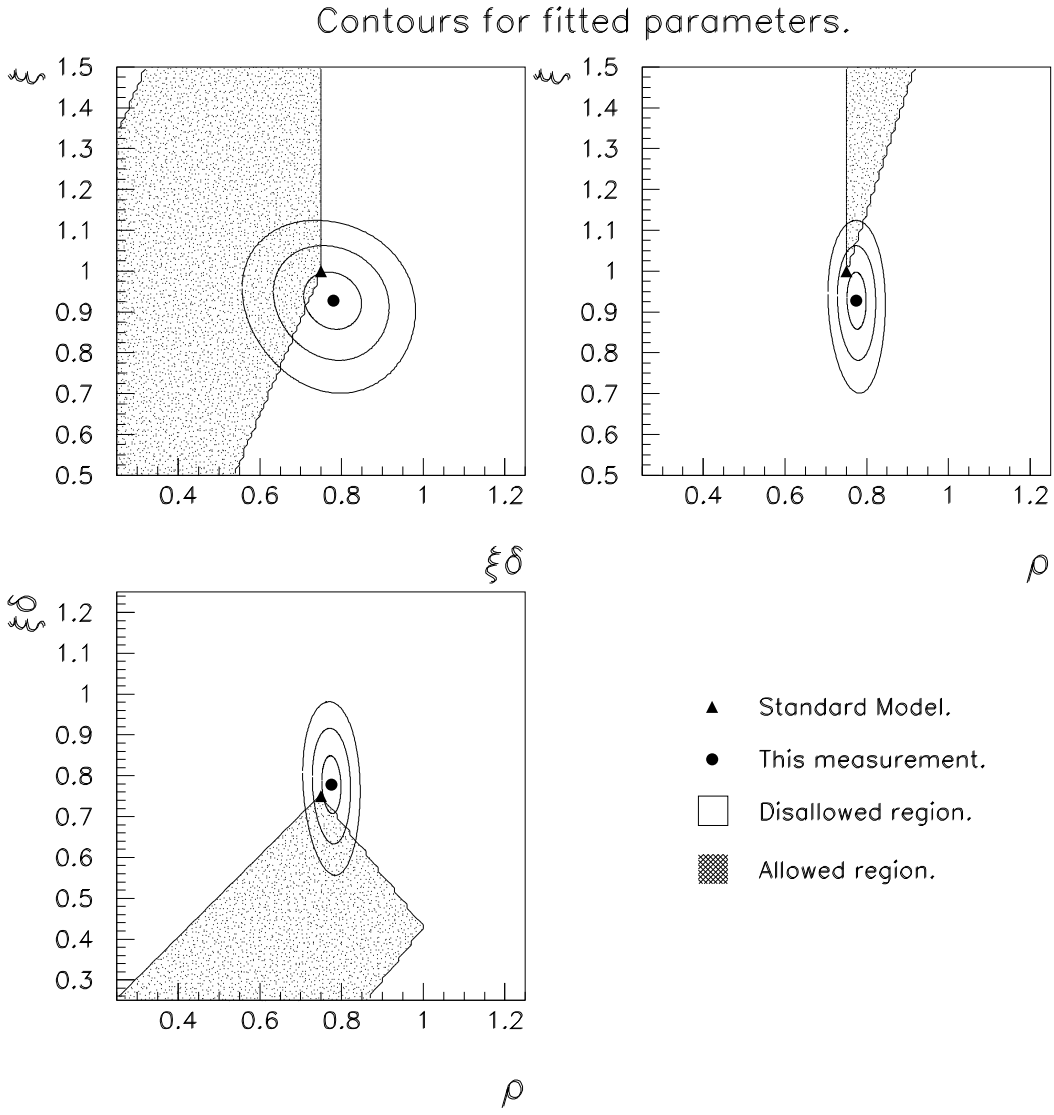

Figure 8: The contours corresponding to $(log\mathcal{L}+\frac{i^2}{2})$, where $i = 1, 2, 3$, for the six parameter fit. In forming the contours the likelihood function is minimised with respect to the other four parameters in the fit.

$$\begin{aligned} h_{\nu_\tau} &= -0.995 \pm 0.028 \pm 0.012, \\ \mathcal{P}_\tau &= -0.129 \pm 0.012 \pm 0.008. \end{aligned}$$

The presented measurements show no deviations from the predictions of pure $V - A$ couplings in τ decays.

As mentioned in Section 2 the Michel parameters are restricted by boundary conditions. The physically allowed regions for various pairs of the parameters ρ, ξ and $\xi\delta$ are shown in figure 8 along with the experimentally determined values for these parameters (assuming lepton universality). In forming the contours the likelihood function is minimised with respect to the other four parameters in the fit.

8 Extraction of the coupling κ_τ^W

The spectra of the τ decay products were used to extract the parameter κ_τ^W. To estimate the theory prediction of the spectra distortion in the case of $\kappa_\tau^W \neq 0$ the Standard Model Monte Carlo was used with the events re-weighted in the following way. For the generated values of the τ handedness and the final lepton momentum, the value $d\Gamma/dx(x, \kappa_\tau^W)$ was calculated according to equations 16 and 17. The ratio $\frac{d\Gamma/dx(x,\kappa_\tau^W)}{d\Gamma/dx(x,0)}$ was then used as an event weight to produce the Monte Carlo spectrum with non-zero tensor coupling. In the case of the τ multipionic decays equation 20 was used to generate event weights.

The value of the tensor coupling parameter was then extracted from a log likelihood fit to the real data of the Monte Carlo spectra with κ_τ^W as a fit parameter. One dimensional spectra of x were used in the case of leptonic τ decays and the two dimensional spectra of $(\cos\theta^*, \cos\psi)$ for semi-leptonic decays. To increase the sensitivity of the semi-leptonic channel further, the region of reconstructed invariant mass between 0.3 and 1.7 GeV was divided into five bins and the fit was performed in each bin simultaneously. This reduced the statistical error of the fit by about 10%. The region of invariant mass below 0.3 GeV was not used because it was dominated by $\tau \to \pi\nu_\tau$ decays which have no sensitivity to the tensor coupling.

The illustration for the channel $\tau \to \mu\overline{\nu}_\mu\nu_\tau$ is given in figure 9 which shows the difference between the real data and the Standard Model Monte Carlo prediction. Also shown is the difference between the best fit Monte Carlo and the Standard Model Monte Carlo. The systematic uncertainty received contributions from the limited Monte Carlo statistics, the background level uncertainty, the variation of spectrum binning, the momentum scale uncertainty for tracks and photons, misidentification of $\tau \to \rho\nu_\tau$ candidates as $\tau \to \pi\nu_\tau$ and the uncertainties in the world average values of the τ branching ratios.

The results of the fits for different decay channels were the following:

$$\begin{aligned}
\tau \to e\overline{\nu}_e\nu_\tau &: \kappa_\tau^W = +0.162 \pm 0.078 \pm 0.030, \\
\tau \to \mu\overline{\nu}_\mu\nu_\tau &: \kappa_\tau^W = -0.043 \pm 0.057 \pm 0.032, \\
\tau \to h(n\pi^0)\nu_\tau &: \kappa_\tau^W = -0.122 \pm 0.059 \pm 0.025.
\end{aligned}$$

Combining these gave

$$\kappa_\tau^W = -0.029 \pm 0.036 \pm 0.018,$$

where the first uncertainty is statistical and the second is systematic.

9 Conclusions

A precise measurement of the Michel parameters and the ν_τ helicity has been presented, together with limits on the anomalous tensor coupling. All the presented results are consistent with the Standard Model. The $V - A$ assumption is however still not fully verified. With the introduction of future B factories the full determination of the Lorentz structure of the τ will be possible.

One can use the measured value of P_R^τ to place limits on five of the complex coupling constants. Following the Bayesian approach (discussed in [32]), only allowing the value

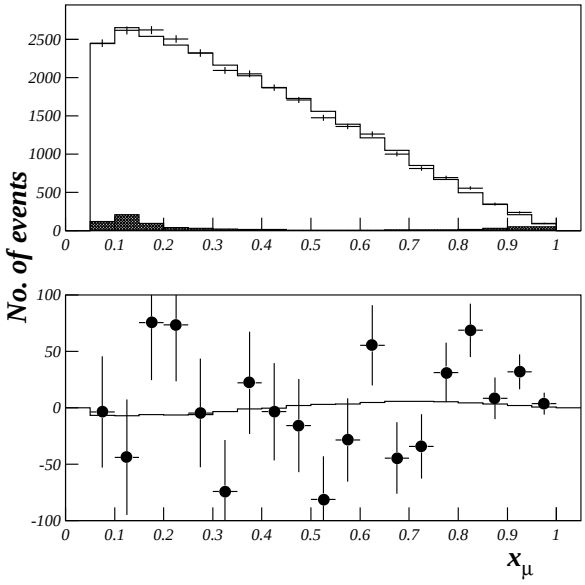

Figure 9: An illustration of the fit to the tensor coupling parameter using the decay $\tau \to \mu\overline{\nu}_\mu\nu_\tau$. Upper plot: spectra of the normalised muon momentum for data (points with error bars), background (hatched) and the best fit Monte Carlo (solid line). Lower plot: the difference between the measured spectrum and the Standard Model prediction (points with error bars); the solid line shows the difference between the best fit Monte Carlo and the Standard Model Monte Carlo.

of P_R^τ to be between 0 and 1, the limit placed on the 'reduced couplings' (defined in section 2), $f^i_{\alpha\beta}$, was $f^i_{\alpha\beta} < 0.312$ at 90% CL. The other couplings are not constrained by the measurement of P_R^τ.

The measured value of η_l can be used to place limits on the mass of the charged Higgs, $M_{H^\pm}$, in extensions to the Standard Model [14, 33]. The τ and the lepton in such models are righthanded. The charged Higgs bosons are therefore represented by the g^S_{RR} coupling. From the one parameter fit to η_l:

$$M_{H^\pm} > 1.08 \times tan\beta \text{ GeV at 90\% C.L.}$$

where $tan\beta$ is the ratio of the vacuum expectation values of the neutral components of the two charged Higgs fields. This limit is obtained using a Bayesian approach in that the value of η_l is constrained to be less than zero.

Unless $tan\beta$ has an unexpectedly large value, this limit is clearly not competitive with those from direct searches.

The measured value of the anomalous tensor coupling, κ_τ^W corresponds to a 90% allowed interval of $-0.095 < \kappa_\tau^W < 0.037$.

Acknowledgements

We are greatly indebted to our technical collaborators, to the members of the CERN-SL Division for the excellent performance of the LEP collider, and to the funding agencies for their support in building and operating the DELPHI detector.
We acknowledge in particular the support of
Austrian Federal Ministry of Science and Traffics, GZ 616.364/2-III/2a/98,
FNRS–FWO, Belgium,
FINEP, CNPq, CAPES, FUJB and FAPERJ, Brazil,
Czech Ministry of Industry and Trade, GA CR 202/96/0450 and GA AVCR A1010521,
Danish Natural Research Council,
Commission of the European Communities (DG XII),
Direction des Sciences de la Matière, CEA, France,
Bundesministerium für Bildung, Wissenschaft, Forschung und Technologie, Germany,
General Secretariat for Research and Technology, Greece,
National Science Foundation (NWO) and Foundation for Research on Matter (FOM), The Netherlands,
Norwegian Research Council,
State Committee for Scientific Research, Poland, 2P03B06015, 2P03B03311 and SPUB/P03/178/98,
JNICT–Junta Nacional de Investigação Científica e Tecnológica, Portugal,
Vedecka grantova agentura MS SR, Slovakia, Nr. 95/5195/134,
Ministry of Science and Technology of the Republic of Slovenia,
CICYT, Spain, AEN96–1661 and AEN96-1681,
The Swedish Natural Science Research Council,
Particle Physics and Astronomy Research Council, UK,
Department of Energy, USA, DE–FG02–94ER40817.

References

[1] L. Michel, Proc. Phys. Soc. A63 (1950) 514;
C. Bouchiat and L. Michel, Phys. Rev. 106 (1957) 170.

[2] ARGUS Coll., H. Albrecht et al, Phys. Lett B 228 (1989) 274;
ARGUS Coll., H. Albrecht et al, Phys. Lett. B 246 (1990) 279;
ARGUS Coll., H. Albrecht et al, Phys. Lett. B 316 (1993) 609;
ARGUS Coll., H. Albrecht et al, Phys. Lett. B 341 (1995) 441;
ARGUS Coll., H. Albrecht et al, Phys. Lett. B 349 (1995) 576.

[3] CLEO Coll., R. Ammar et al, Phys. Rev. Lett. 78 (1997) 4686;
CLEO Coll., T. Coan et al, Phys. Rev. D55 (1997) 7291;
CLEO Coll., J. Alexander et al, Phys. Rev. D56 (1997) 5320.

[4] ALEPH Coll., D. Buskulic et al, Phys. Lett. B 346 (1995) 379.

[5] L3 Coll., M. Acciari et al, Phys. Lett. B 377 (1996) 313;
L3 Coll., M. Acciari et al, Phys. Lett. B 438 (1998) 405.

[6] OPAL Coll., K. Ackerstaff et al, Measurement of the Michel parameters in leptonic τ decays, CERN-EP/98-104 (1998).

[7] SLD coll., K. Abe et al,Phys. Rev. Lett. 78 (1997) 4691.

[8] F. Scheck, Leptons, hadrons and nuclei, North Holland, Amsterdam, 1983.

[9] K. Mursula and F. Scheck, Nucl. Phys. B253 (1985) 189-204.

[10] K. Mursula, M. Roos and F. Scheck, Nucl. Phys. B219 (1983) 321.

[11] W. Fetscher, Leptonic τ decays: How to determine the Lorentz structure of the charged leptonic weak interaction by experiment. Phys. Rev. D42, (1990) 1544.

[12] W. Lohmann, J. Raab, Charged current couplings in τ decays, DESY 95-188 (1995).

[13] W. Hollik and T. Sack, Phys. Lett. B284 (1992) 427.

[14] A. Stahl, Phys. Lett. B 324 (1994) 121.

[15] A.Pich and J.P.Silva: Phys. Rev. D52 (1995) 4006.

[16] T. Kinoshita, A. Sirlin, Phys. Rev. 108 (1957) 844.

[17] M. Davier, L. Duflot, F. Le Diberder, A. Rougé, Phys. Lett. B 306 (1993) 411.

[18] V. N. Bolotov et al. Phys. Lett. B243 (1990) 308

[19] S. A. Akimenko et al. Phys. Lett. B259 (1991) 225

[20] A. Poblaguev, Phys. Lett. B238 (1990) 108;
M. V. Chizhov, Mod. Phys. Lett. A8 (1993) 2753

[21] M. V. Chizhov, hep-ex/9612399

[22] DELPHI coll., P. Abreu et al, Nucl. Inst. and Meth., A303 (1991) 233;
DELPHI coll., P. Abreu et al, Nucl. Inst. and Meth., A378 (1996) 57.

[23] "DELSIM Reference Manual", DELPHI Note 89-68, Sept. 1989, (unpublished).

[24] S. Jadach et al., Comp. Phys. Comm. 79 (1994) 503.

[25] J. E. Campagne and R. Zitoun, Z. Phys. C43 (1989) 469.

[26] F. A. Berends, W. Hollik and R. Kleiss, Nucl. Phys. B304 (1988) 712.

[27] T. Sjöstrand, Comp. Phys. Comm. 27 (1982) 243, ibid. 28 (1983) 229;
T. Sjöstrand and M. Bengtsson, Comp. Phys. Comm. 43 (1987) 367;
T. Sjöstrand, "PYTHIA 5.6 JETSET 7.3 Physics and Manual", report CERN-TH 6488/92 (1992).

[28] F. A. Berends, P. H. Daverveldt, R. Kleiss, Phys. Lett. B148 (1984) 489;
Comp. Phys. Comm. 40 (1986) 271.

[29] P. Seager, "A measurement of the Michel parameters and the ν_τ helicity in τ lepton decays using the DELPHI detector at LEP", PhD Thesis, Lancaster University, RAL-TH-1998-011 (1998).

[30] M. Schmidtler, A convenient parameterisation for the general matrix element of leptonic tau decay, University Karlsruhe Preprint IEKP-KA/93-14, (1993).

[31] DELPHI 98-100, CONF 168, 22 June 1998.

[32] M. Aguilar-Benitez et al., Review of Particle Properties, Phys. Rev. D54 (1996) 21.

[33] H. E. Haber, G. L. Kane and T. Sterling, Nucl. Phys. B161 (1979) 493